CHAPTER 20

WAVE DIRECTION COMPUTATIONS WITH THREE GAGE ARRAYS

by

D. Esteva[1]

INTRODUCTION. Wave direction is an important parameter in the solution of many coastal engineering problems such as the estimation of sediment transport and the response of coastal structures. Wave-gage arrays are among the most widely proposed systems for measuring wave direction. In late March 1970, the U.S. Army Coastal Engineering Research Center (CERC) installed an array of five pressure sensors off the California coast.

Figure 1 gives the location of the array, its geometry and dimensions. The water depth at the site was approximately 9.14 meters (30 feet) and the gages were positioned .76 meters (2.5 feet) from the bottom.

One use for the array data would be to compare redundant values of wave direction and estimate the level of accuracy of the computations. Redundant values of direction were obtained from the ten three-gage arrays possible with five gages. Three-gage arrays offer some advantages over arrays involving a larger number of gages and have been proposed by many investigators. An obvious advantage involves economics. Non-linear arrays offer the advantage over linear arrays that straight forward mathematical expressions can be derived for the unambigous computation of direction. These expressions involve the phase differences between gage pairs for the waves present, no recourse to two-dimensional spectral analysis is necessary. However, it is necessary to assume long and relatively straight crested waves, traveling in well determined directions, and geometrically stationary over the array. The first two assumptions are supported by high altitude aerial photographs, Figure 2 and, by radar scans of the wave field, Figure 3. Fujinawa (1975) conjectures that narrow directional spread is responsible for the incomplete recovery of the true directional spectrum from field records in his computations using high directional resolution.

Direction estimates for all bands .01 hz wide between approximately 30 and 3 seconds were obtained from the ten arrays using cross spectra between gage pairs. The lower limit on period is estimated from the water column over the pressure sensors. The resulting directions at bands of maximum energy disagreed by 20^{o} to 160^{o}. It had been expected that the array would yield directions to hetter than 20^{o}.

---

[1]Mathematician/Oceanographer, U.S. Army Coastal Engineering Research Center, Ft. Belvoir, VA

The computational model was applied to computer simulated narrow-banded wave trains propagating across the array. Because of the narrow-bandedness of the simulated trains, the frequency resolution used in these computations was increased to approximately .001 hz. It was found that the directional results depend highly on the spectral width, both, in frequency and direction, of the wave train involved and on the relationship between wavelength at the site and gage separations.

The same higher frequency resolution was used to analyze field wave pressure records having standard deviations above 2 feet. Average discrepancies of 20 degrees among computed directions were obtained for narrow-banded trains with periods longer than 10 seconds. Larger discrepancies resulted for shorter periods. Thus, accuracies no better than 20 degrees can be expected for wave directions resulting from three-gage arrays.

ARRAY OPERATION AND DATA SUMMARY. The gages in the array were developed mostly at CERC. The heart of the system is a Fairchild pressure transducer which is potted inside a two-inch plexiglass tube, (Williams 69, Peacock 74). A plastic tube filled with silicone oil transmits the sea water pressure to the transducer. A rubber diaphram separates the silicone oil from the sea water. A teflon scouring pad dipped in anti-fouling paint separates this rubber diaphram from the end of the package which admits the sea water pressure. The instrument is mounted vertically on a tripod. The signals from the pressure transducers are brought by cables to a recording and transmitting station on shore.

The water pressure at each of the five gages was registered continuously at four samples per second on digital magnetic tape. The recording proceeded with few interruptions during most of 1970. It can be shown (Kinsman, 1965), that the potential energy in the wave field is proportional to the variance of the time history of sea surface elevation at a fixed location. This energy is also proportional to the square of the wave height. Thus, the standard deviation of sea surface elevations (or of the pressure at a certain depth) is a good measure of wave height. Four times the standard deviation approximately equals the significant wave height.

The standard deviation of the wave pressure in each gage was computed for observations consisting of simultaneous 20-minute recordings. The mean standard deviation was found for each observation. Table 1 gives a breakdown of the largest difference of individual standard deviations in an observation from their mean for 871 observations processed in 1970 regardless of magnitude. This breakdown indicates the system operated in a consistent way. The field wave records used for computing wave direction were chosen from those observations in this Table for which the standard deviations in the five gages differed by 3% or less from their mean and for which the uncompensated significant wave height was above 2 feet.

TABLE 1. PERCENT OF OBSERVATIONS FOR WHICH THE LARGEST DEVIATION OF INDIVIDUAL STANDARD DEVIATION IN THE OBSERVATION FROM THEIR MEAN WAS AS INDICATED. EIGHT-HUNDRED AND 71 OBSERVATIONS IN 1970.

Deviation from mean	Percent of Observations
$\leq$ 2%	41
(3 - 10%)	52
(11 - 20%)	1
$\geq$ 20%	6

COMPUTATION OF WAVE DIRECTION

For a long crested sinusoidal wave with frequency σ_i, propagating in direction α_i, the phase difference between locations 1 and 2 with coordinates (x_1,y_1) and (x_2,y_2) respectively, is given by:

$$\Phi_{12} = K_i [(x_1-x_2) \cos\alpha_i + (y_1-y_2) \sin\alpha_i] \quad (1)$$

where $K_i = 2\pi/L_i$, is the wave number associated with frequency σ_i, and L_i is the wave length.

Expressions for the phase differences between two pairs of gages in a three-gage array allow solving for the sine and cosine of the direction of wave travel α_i. Thus the angle is determined uniquely. Estimates of a representative phase difference between gage pairs for bands of constant frequency width are easily computed from cross-spectra of the wave (pressure) records. These spectra give average values of the covariance of the wave records along two perpendicular directions for each band. The expediency in these computations is appealing provided the resulting directions are of engineering value.

The co-spectrum (Co) and quad spectrum (Quad) may be defined as, (Jensen and Watts, 1968):

$$Co_\Delta = \sum_\Delta X_1 X_2 \cos \phi_{12}$$

$$Quad_\Delta = \sum_\Delta = X_1 X_2 \sin \phi_{12}. \quad (2)$$

where X_1 and X_2 are the frequency spectral estimates from wave records 1 and 2 and the $\sum_\Delta$ indicates summation over the adjacent spectral periods combined

to make up a band. The representative phase difference for the band is given by expression 3 below, where the sign of numerator and denominator must be taken into account.

$$\phi_{12_\Delta} = \tan^{-1}\left[\frac{\text{Quad}_\Delta}{\text{Co}_\Delta}\right] \tag{3}$$

Cross spectra between gage pairs were computed for bands approximately .01 hz wide for a few observations. A representative wave direction was computed for each band between 30 and 3 seconds for the 10, arrays. The agreement among these redundant values is an indication of the degree of confidence that can be placed on the resulting directions.

Disagreements on the order of 20^o were obtained for bands of maximum energy with central periods above 10 seconds. For bands with maximum energy at shorter central periods disagreements on the order of 160^o were obtained.

It had been expected that the array would yield directions to better than 20 degrees and for periods between 25 and 7 seconds.

SIMULATED OBSERVATIONS

To gain understanding of the problems involved, wave records arising from narrow-banded wave trains propagating through the array in a specified direction were simulated in the computer. Each simulated observation consisted of values of the wave profile at the five locations computed at 1/4 second intervals for slightly over 17 minutes (1024 seconds) to simulate the sampling rate and record duration customarily used at CERC for the field data.

Fast Fourier Transform (Cooley and Tukey 196.7) computations yield the contribution to the variance at each of a set of frequencies ω_m's, which are harmonics of a fundamental given by the inverse of the record duration, T. The frequencies of these harmonics will be referred to as *spectral frequencies* and the corresponding periods, given by their inverse the *spectral periods*. The resulting spectrum will be termed the *high resolution spectrum*. For records 1024 seconds in duration, this high resolution approximately equals .001 hz.

Assume a sinusoid with frequency given by

$$\sigma = \frac{2\pi(\hat{m} + \delta)}{N\Delta t} \tag{4}$$

where Δt is the interval of time between samples and δ is less than or equal to 1/2. This expression provides for assigning frequencies which

differ from the spectral frequencies. The contribution to the variance at the spectral frequencies, of the sampled record is given by:

$$S_m^2 = a_m^2 + b_m^2 \qquad m = 1, \ldots, N/2 \tag{5}$$

where a_m and b_m are the Fourier coefficients. Harris shows (Harris 1974) that for values of m near $\hat{m}$; i.e., for ω_m near the frequency of the sinusoid, and for $\hat{m}$ far removed from one and N/2, the expressions below are good approximations to the coefficients.

$$a_m \doteq \frac{A \sin \pi\delta \cos(\phi - \pi\delta)}{\pi(\hat{m} - m + \delta)}$$

$$b_m \doteq \frac{A \sin \pi\delta \sin(\phi - \pi\delta)}{\pi(\hat{m} - m + \delta)} \tag{6}$$

It is clear that slow convergence of the energy toward the spectral period closest to the assigned period is indicated. Thus the energy is spread over adjacent spectral periods. This spreading, due to the fineteness of the record is usually referred to as spillover.

The technique routinely used at CERC to decrease spillover is to apply the cosine bell data window as indicated below:

$$\hat{Y}_i = \frac{1}{2}\left(1 - \cos\frac{2\pi t_i}{T}\right) Y_i \qquad i = 1, \ldots\ldots N \tag{7}$$

where Y_i are the values in the original record. The Fourier coefficient for the resulting $\hat{Y}_i$ are given by:

$$\hat{a}_m \doteq \frac{A \sin \pi\delta \cos(\phi - \pi\delta)}{2\pi(\hat{m} - m + \delta)\left[(\hat{m} - m + \delta)^2 - 1\right]}$$

$$\hat{b}_m \doteq \frac{A \sin \pi\delta \sin(\phi - \pi\delta)}{2\pi(\hat{m} - m + \delta)\left[(\hat{m} - m + \delta)^2 - 1\right]} \tag{8}$$

Thus convergence is greatly increased and spillover is effectively reduced to three adjacent spectral periods.

The cosine bell data window was applied to all records discussed here. Thus, in simulating records it was sufficient to consider wave trains consisting of three sinusoids with nearby periods spread over at most six adjacent spectral periods. Central periods near 16 and eight seconds were chosen to simulate a relatively long period swell and a shorter period swell. Swells with these periods are common in the West Coast.

Figures 4 and 5 are plots of the high resolution spectra for two of the simulated observations. Energy density at each spectral frequency is plotted versus a linear frequency scale in hz. The corresponding period values are given along the top axis. All of the spectral plots shown here have been plotted in the same way and to the same scale. The spectra in these two figures resulted from combining only three sinusoids; yet, energy contributions appear at from five to nine adjacent periods. In Figure 4 three relative maxima separated by two minima can be identified. The energy shown at these two minima may be interpreted as due to spillover since no sinusoids were combined with the appropriate periods.

Energy minima can easily be identified in the high resolution spectra of field wave observations. The energy at these minima may be used as a measure of spillover and noise in these spectra.

Table 2 gives the characteristics of the first eight simulated observations and Table 3 the computational results at spectral periods closests to the assigned periods.

The last column in Table 3 gives the average resulting directions from the ten arrays. For wave trains 1 thru 3 the computed directions agree for the ten arrays and with the input directions to within 1 degree. Directional results for wave train No. 4 are correct only for spectral period number 62. The main difference between this train and No. 2is the narrower spectral width. Wave train No. 2 gave the correct direction for all spectral periods while No. 4 did not.

Directional results seem meaningless for simulated wave trains 5 through 8. To determine whether these poor results were due to some programming deficiency another eight sets of simulated records were generated interchanging periods and directions.

The directional results for the sinusoids with periods clustered around 16 seconds were of the same quality regardless of the assigned direction. The directional results for the 8 second sinusoids, however, indicate that the capability to sense the correct direction for these shorter waves depends on the orientation of the three-gage array relative to the direction of propagation of the incoming wave. This is not surprising when it is realized that the effective gage separation for the different gage pairs varies with this relative orientation.

Additional simulated records were generated using the same periods as for observation No. 5 but assigning the additional directions listed in

Table 4. At the top of each column the orientation and shape of the corresponding array is given. Computed directions omitted differed by 87° and more from the assigned directions listed on the left hand column. It is apparent from Table 4 that the more nearly equilateral arrays give correct directions for a wider range of periods.

TABLE 2. CHARACTERISTICS OF SIMULATED WAVE TRAINS

Wave Train	Period (sec)	Amp. (cm)	Direction (degrees)
1	16.75..	11.43	21 S
	15.97...	15.24	21 S
	15.25...	11.43	21 S
	16.75..	11.43	21 S
2	15.97...	15.24	15 S
	15.25...	11.43	21 N
	16.48..	11.43	21 S
3	15.97..	15.24	21 S
	15.72..	11.43	21 S
	16.48..	11.43	21 S
4	15.97..	15.24	21 N
	15.72..	11.43	21 N
	8.18..	11.43	60 N
5	7.99..	15.24	60 N
	7.80..	11.43	60 N
	8.18..	11.43	60 N
6	7.99..	15.24	40 N
	7.80..	11.43	60 S
	8.11..	11.43	60 N
7	7.99..	15.24	60 N
	7.93..	11.43	60 N
	8.11..	11.43	60 N
8	7.99..	15.24	40 N
	7.93..	11.43	60-S

The effect of angular spread in the 16 second wave train was investigated by introducing angular spreads among assigned directions and keeping frequency separations among sinusoids constant (three spectral frequencies). Input angular spreads of 5°, 10°, and 20° gave rise to angular spreads of 0°, 16°, and 32° respectively.

FIELD WAVE OBSERVATIONS

To better evaluate directional results from field observations, spectral periods at or near which wave trains may be present in the field were isolated in the high resolution spectra of 44 field observations. The

average uncompensated significant wave height in each observation was over two feet and discrepancies of individual standard deviations from their mean was 3% or less.

TABLE 3. COMPUTATIONAL RESULTS AT CLOSEST SPECTRAL FREQUENCIES FOR SIMULATED WAVE TRAINS

Wave Train	Closest Spectral Frequency (1/024 hz)	Spectral Period (sec)	Amp. (cm)	Direction (degrees)
	61	16.79	5.62	20 S
1	64	16.00	7.55	20 S
	67	15.28	5.70	20 S
	61	16.79	5.62	21 S
2	64	16.00	7.55	15 S
	67	15.28	5.70	20 N
	62	16.52	5.52	20 S
3	64	16.00	5.35	20 S
	65	15.75	1.19	20 S
	62	16.52	5.52	21 S
4	64	16.00	5.35	25 S
	65	15.75	1.19	36 N
	125	8.19	5.62	142 N
5	128	8.00	7.55	142 N
	131	7.82	5.70	142 N
	125	8.19	5.62	142 N
6	128	8.00	7.55	78 N
	131	7.82	5.70	162 S
	126	8.13	5.52	142 N
7	128	8.00	5.35	142 N
	129	7.94	1.19	142 N
	126	8.13	5.52	142 N
8	128	8.00	7.14	76 N
	129	7.94	5.83	172 S

Plots of the high resolution spectra for these observations will be published in a CERC Technical Report. Figures 6 and 7 are shown here to illustrate the two typical spectral shapes obtained. The spectra on Figure 6 show most of the energy between approximately 13 and 18 seconds. The

Three-Gage Arrays

Assigned Direction Degrees	1-2-3	1-2-4	1-2-5	1-3-4	1-3-5	1-4-5	2-3-4	2-3-5	2-4-5	3-4-5
										
60 N				59 N	60 N	59 N		60 N		60 N
40 N	40 N	40 N	40 N	40 N	40 N	40 N		40 N		39 N
21 N	21 N	20 N	21 N	21 N	20 N	20 N		21 N		20 N
15 N	14 N	14 N	14 N	14 N	14 N	14 N		14 N		15 N
15 S	14 S	14 S		14 S			14 S	14 S	14 S	15 S
21 S	21 S	20 S		20 S			20 S	20 S	20 S	20 S
40 S	40 S	39 S		39 S			39 S	40 S	39 S	39 S
60 S				60 S			60 S	59 S	59 S	60 S

Table 4 Directional results of high resolution spectral computations for 8 second wave.

Results differing by 87° or more from the assigned directions on the left hand column have been omitted.

structure suggests more than one wave train present in that period range. The spectra in Figure 7 display bimodality - a large portion of the energy appearing at shorter periods. A "background" energy was estimated for each observation by systematically averaging the energy at minima between 25 and seven seconds in the spectrum. Adjacent spectral periods in this range showing energy content twice the background or above were identified and considered arising from the same wave train. The number of adjacent periods in each train was used as a measure of the *spectral width* of the train. The energy had to be above the chosen level at all five gages for the spectral period to be included in the group. The spectral period among these showing maximum energy was taken as the "period" of the wave train.

Directions were computed at all the spectral periods in each train for the ten arrays. The total spread among these directions was found; and, an average total spread was computed for trains having the same spectral width. The same was done for the spread in computed directions at the "period" of the train.

Twenty-five percent (25%) of the identified wave trains had total directional (computed) spreads above 100^{o} and were not considered any further. For 89% of the discarded trains, the "period" of the train was under 9.4 seconds. Thus trains with "period" under this value were also discarded.

Table 5 shows the results for the different spectral widths for the 280 trains retained.

TABLE 5. AVERAGE SPREAD IN COMPUTED DIRECTIONS FOR 280 WAVE TRAINS IDENTIFIED IN THE HIGH RESOLUTION SPECTRUM OF 44 FIELD WAVE OBSERVATIONS

Spectral Width (hz)	Average Total Spread in Direction (for all Periods) (Degrees)	Average Spread in Direction for "Period" of Train (Degree)	No. of Cases
.001		21.8	96
.002	30.9	22.9	58
.003	33.6	20.2	41
.004	41.5	20.4	22
.005	38.7	19.8	21
.006	43.8	19.8	16
.007	48.2	17.0	5
.008	84.5	17.6	8
.009	53.0	15.3	6
.010	49.3	13.7	3
.011	38.0	18.0	1
.012	81.0	15.0	1
.013	48.5	15.2	2

These results indicate that narrow peaks consisting of from one to three spectral periods are most frequent. The total spread in direction increases with frequency width. The spread in the direction at the "period" of the train remains relatively constant. Since the average spread at this "period" for narrow-banded trains ($\leq$ .003 hz) is 21.8 degrees; it is to be expected that three-gage arrays cannot yield directional results to any better accuracy.

There are various possible explanations for the large spreads observed in the directions computed from field records. For the long crested wave model to be applicalbe, it is important that:

- The phase differences be known accurately or that the probable error in their computed values be known;
  from expressions 6 and 8 it is clear that the analysis yields accurate phase differences for strictly monochromatic conditions. For each component with nearby period in a wave train the value of δ in expressions 6 (or 8) will be different; thus, no accurate value of the phase difference for the train nor of the error involved can be estimated;

- the wave crests over the array site be long and straight;
  waves with periods between 20 and eight seconds had and are undergoing refraction at the site of the array; thus, their crests are not exactly straight; for the longer waves, with wave lengths at the array site several times the gage separations, the curvature will not introduce much error; this is not the case for the shorter waves, and orientation of the array becomes important;

- the sea surface be stationary in time for the duration of the record, and in space over the span of the array.
  Stationarity of the wave field is assumed in most wave directional models. The extent and frequency of its applicability either in the open ocean or in coastal waters has not been established.

These three factors are sufficient to account for the discrepancies found in computed directions.

CONCLUSIONS

The results of directional computations both for simulated and field wave data records indicate three-gage arrays have some capability to determine wave direction under certain conditions. This capability depends on:

- the dimension of the array and the water depth at the site which

place a lower limit on the wave period for which possibly accurate directions may be computed;

- o the orientation of the array for the shorter periods;
- o the nature of the wave field; directional results for wave trains with a narrow frequency districution and/or for which the computed directions differ little at adjacent spectral periods might be meaningful.

For wave trains with narrow frequency and directional spreads; and, period above 10 seconds, the Pt. Mugu arrays yield directions to an estimated accuracy of 20^{o}.

Bibliography

Borgman, L. E. and Panicker, N. N., "Design Study for A Suggested Wave Gage Array off Point Mugu, California," Technical Report HEL 1-14 University of California, Hydraulic Engineering Laboratory, Berkeley, California, January 1970.

Cooley, J. W. and Tukey, J. W., "The Fast Fourier Transform," IEEE Spectrum, Vol. 4, pp 63-70, 1967.

Fujinawa, Yukio, "Measurement of Directional Spectrum of Wind Waves Using An Array of Wave Detectors" - Journal of the Oceanographical Society Of Japan, Vol. 30, pp 10-22, 1974.

Fujinawa, Yukio, "Measurement of Directional Spectrum of Wind Waves Using An Array of Wave Detectors Part II - Field Observations" - Journal of the Oceanographical Society of Japan, Vol. 31, pp 25-42, 1975.

Harris, D. Lee, "Finite Spectrum Analyses of Wave Records," International Symposium on Ocean Wave Measurement and Analysis, September 9-11, 1974, New Orleans, Louisiana.

Jenkins and Watts, "Spectral Analysis and Its Applications," Holden-Day, 1968.

Kinsman, B., "Wind Waves," Prentice-Hall, Inc., Englewood Cliffs, New Jersey, 1965.

Peacock, Harold C., "CERC Field Wave Caging Program," Proceedings of the International Symposium on Ocean Wave Measurement and Analysis, September 1974, New Orleans, Louisiana, USA.

Williams, Leo C., Technical Memorandum No. 30, U.S. Army Corps of Engineers, Coastal Engineering Research Center, December 1969.

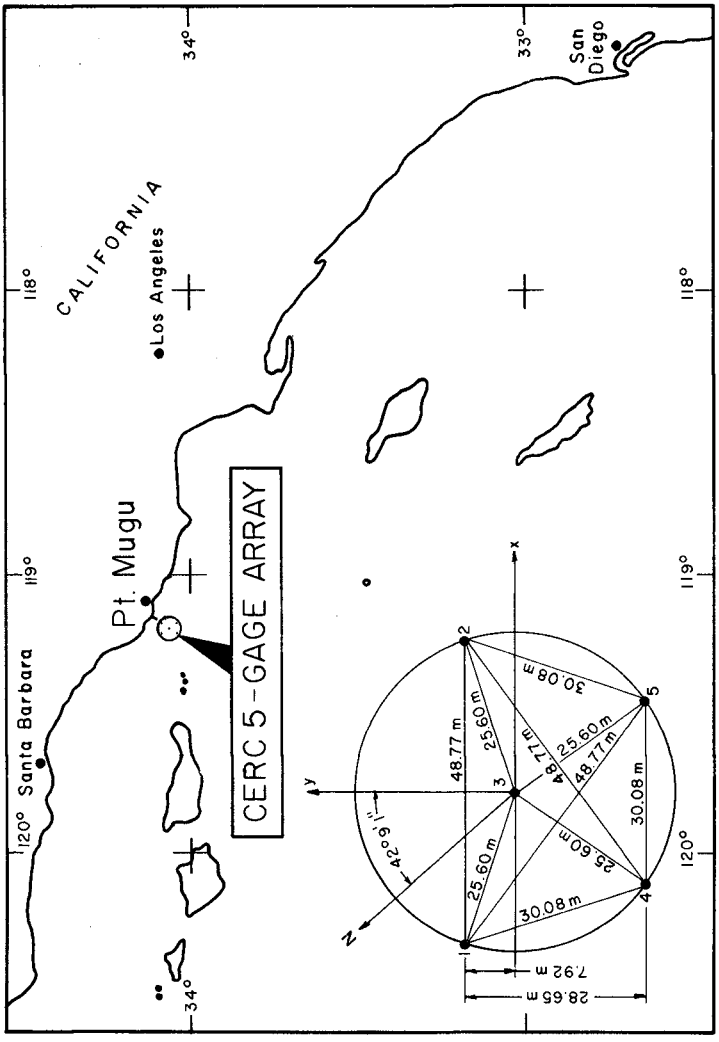

FIGURE 1. LOCATION, GEOMETRY, AND DIMENSIONS OF FIVE-GAGE ARRAY.

FIGURE 2. AERIAL PHOTO OF WAVE FIELD. PT. SAINT GEORGE, CALIFORNIA.

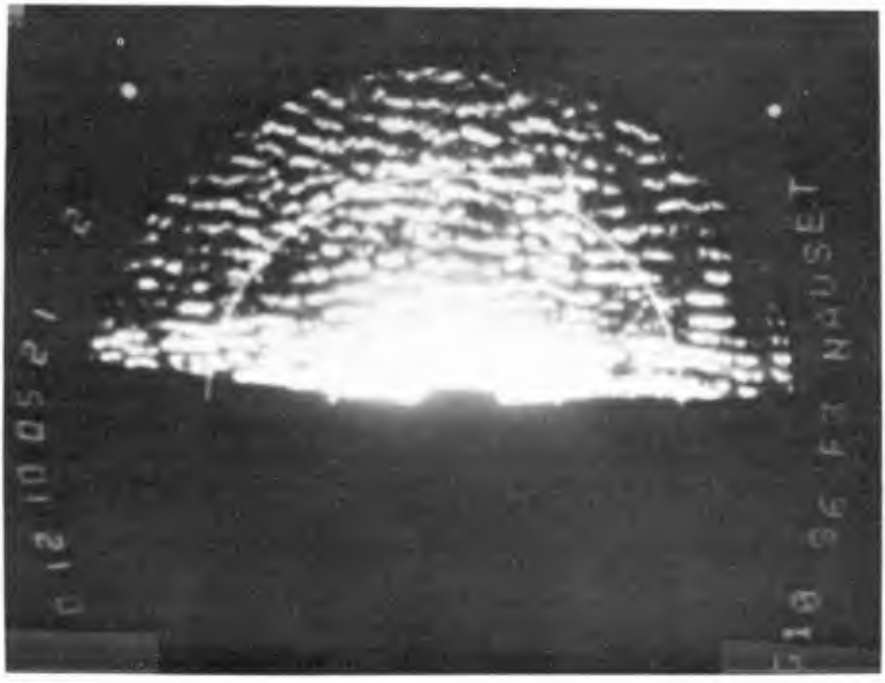

FIGURE 3. RADAR SCAN OF WAVE FIELD AT NAUSET, MASSACHUSETTS.

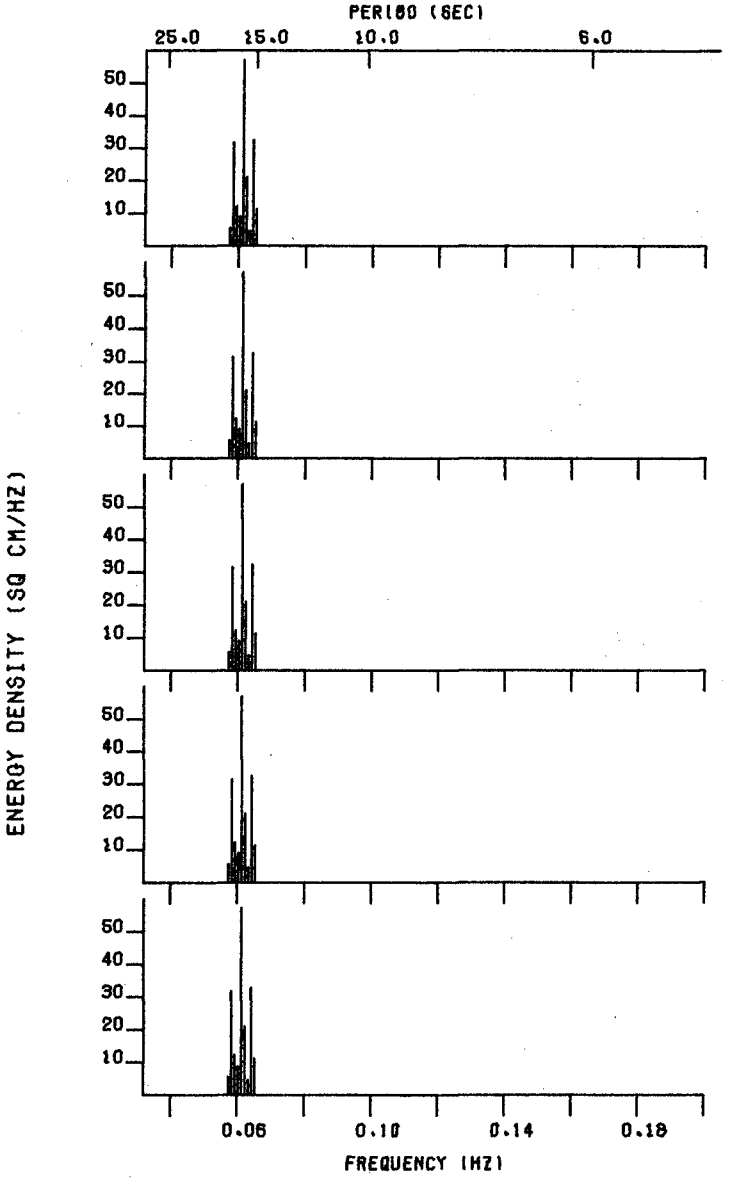

FIGURE 4. HIGH RESOLUTION SPECTRA PRESSURE GAGES ONE THRU FIVE POINT MUGU, CALIFORNIA, SIMULATED OBSERVATION NO. 1.

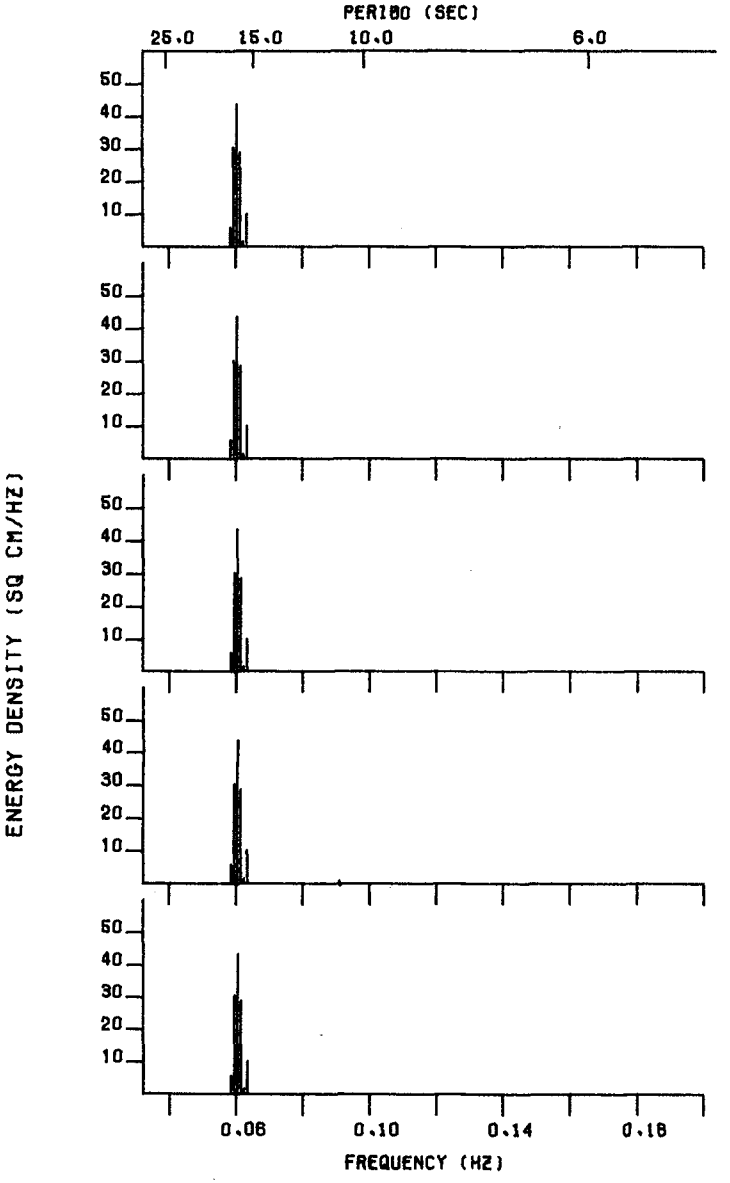

FIGURE 5. HIGH RESOLUTION SPECTRA PRESSURE GAGES ONE THRU FIVE POINT MUGU, CALIFORNIA, SIMULATED OBSERVATION NO. 3.

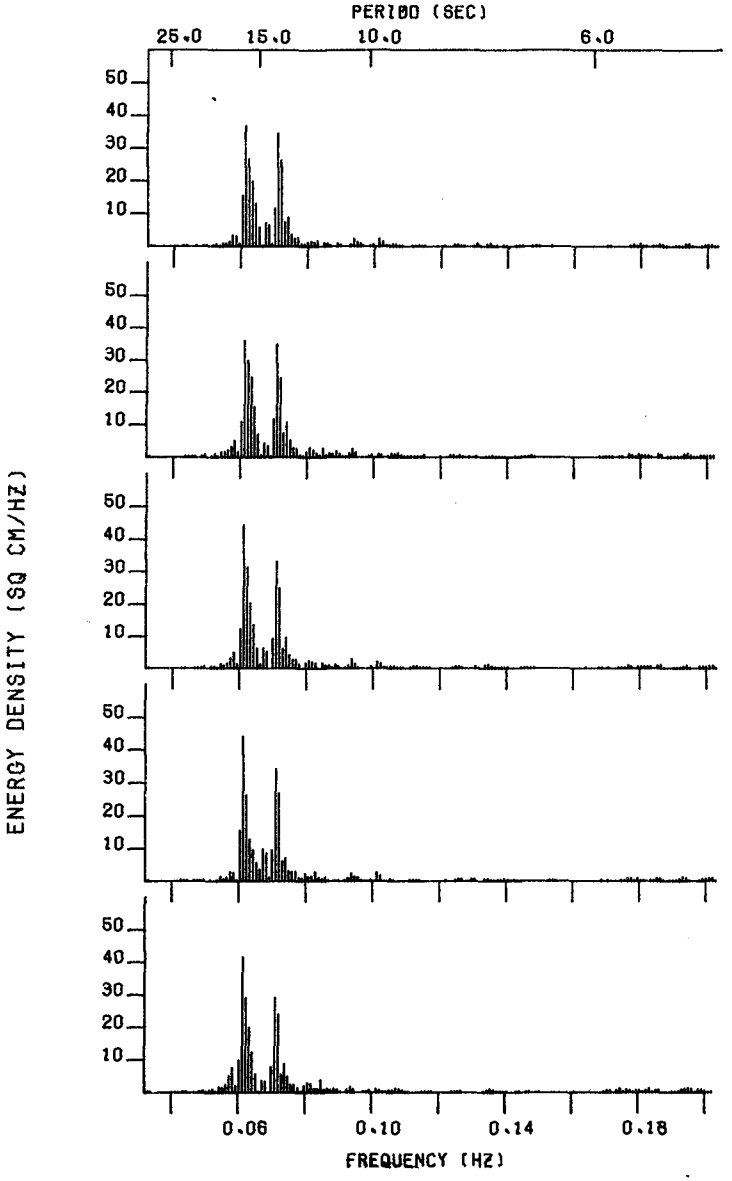

FIGURE 6. HIGH RESOLUTION SPECTRA PRESSURE GAGES ONE THRU FIVE POINT MUGU, CALIFORNIA, 307 HRS. JUNE 25, 1970. SIGNIFICANT WAVE HEIGHT 76.9 CM (2.5 FT)

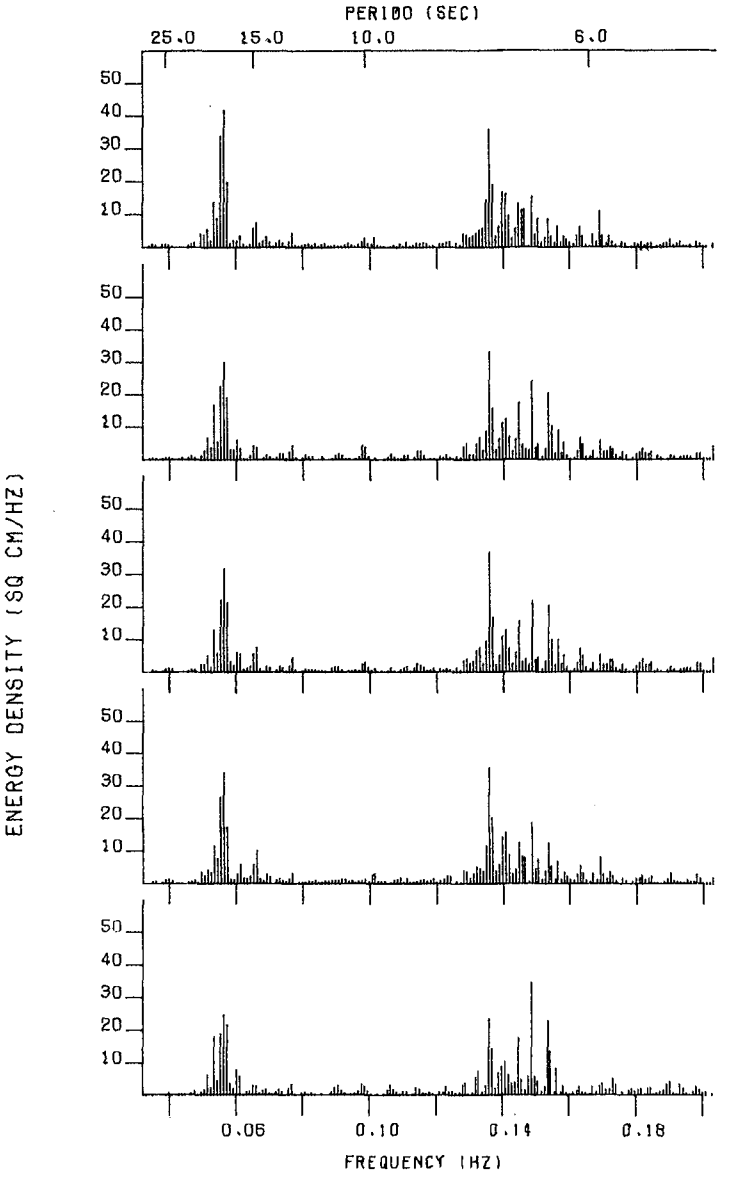

FIGURE 7. HIGH RESOLUTION SPECTRA PRESSURE GAGES ONE THRU FIVE POINT MUGU, CALIFORNIA, 1421 HRS. JUNE 10, 1970. SIGNIFICANT WAVE HEIGHT 109. 3 CM (3.6 FT)